Conformational and phase behavior of comb copolymer brushes

Stepanyan, Roman

CHAPTER 6

Phase Behavior and Structure Formation of Hairy-Rod Supramolecules

Phase behavior and microstructure formation of rod and coil molecules, which can associate to form hairy-rod polymeric supramolecules, are addressed theoretically. Association induces considerable compatibility enhancement between the rod and coil molecules and various microscopically ordered structures can appear in the compatibility region. The equilibria between microphase separated states, the coil-rich isotropic liquid and the rod-rich nematic are discussed in detail. In the regime where hairy-rod supramolecules with a high grafting density appear as a result of the association, three phase diagram types are possible depending on the value of the association energy. In the low grafting density regime only the lamellar microstructure is proven to be stable.

6.1. Introduction

Supramolecular chemistry allows synthesis of highly specific complexes, including hairy-rods, where chemically different groups are connected by means of a reversible bond (see introductory section 1.2.2). In turn, the supramolecules, built in this way, are able to form a hierarchy of structures, resembling in this respect the considered

above covalent hairy-rods. However, the supramolecular systems show much richer phase behavior involving competition between microstructures and homogeneous macrosphases.

In the previous chapter we presented a theoretical analysis of structure formation in melts of hairy-rod polymers (see also [147]). We showed that three different microphases are possible: one lamellar and two hexagonal. If the side chains are long enough for the elastic stretching free energy of the side chains to completely dominate the repulsive interaction between the backbone and the side chains, hexagonally ordered domains of hairy-rod cylindrical brushes are formed. The lamellar state is found to be stable for shorter side chains and occupies an important part of the phase diagram. In the intermediate side chain length regime a hexagonally ordered structure appears characterized by cylindrical micelles with an elongated core cross section and containing several hairy-rod polymers.

Supramolecular hairy-rods represent a more complicated system. Its phase behavior is primarily determined by an interplay between association and chemical incompatibility of the components. In a weakly associating system a macrophase separation should prevail over microstructure formation. In contrast, if the association is strong enough, the appearing supramolecules are expected to self-organize in microstructures, which can be described in terms similar to covalent hairy-rods. Thus, the first objective of this chapter is to address the complex equilibrium in the associating rod – coil system and reveal the conditions, under which the self-organization becomes possible. Further, we aim to consider the competition between appearing micro- and macrophases in order to find their stability regions.

6.2. The model

We consider a melt consisting of rigid rods of length L and diameter d ($L \gg d$) and flexible coils consisting of N beads of volume v and statistical segment length a. The ideal coil size is $R_c = a\sqrt{N}$, $L \gg R_c$. We will assume that each rod contains M associating groups (average distance between two successive groups is $b = L/M$) which can form bonds with the associating end of the coil (Figure 6.1a). It is assumed that each coil has only one associating end. The energy of association between rod and coil equals $-\epsilon$. The concentration of rods in the melt is c and their volume fraction is $f = (\pi/4)Ld^2c$. The interaction between rods and coils can be introduced in the same way as in the previous chapter. It is well known that rods and polymer coils in the molten state are practically incompatible and separate into a nematic

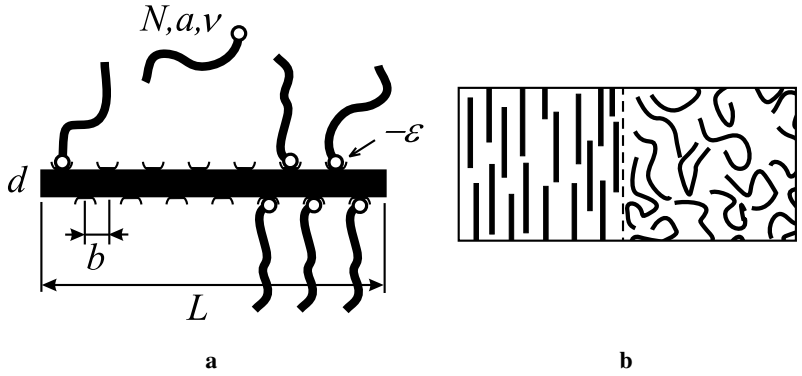

Figure 6.1: (a) Model of the hairy-rod as a stiff backbone with reversibly attached flexible side chains. (b) Flat interface between pure nematic and isotropic phase.

phase consisting of rods and an isotropic phase consisting of the flexible polymer [142, 143]. The interface between the nematic and isotropic phase (Figure 6.1b), is assumed to be sharp and the interfacial tension γ corresponding to the planar orientation of rods at the interface is given by

$$\gamma = (w + sT)/d^2 \,, \tag{6.1}$$

where w is the energetic part of the surface energy and $s > 0$ is the entropic part (here T is temperature in energetic units). According to the definition (6.1), if a rod penetrates into the polymer melt its free energy loss is approximately equal to (c.f. formula (5.1) from the previous chapter)

$$\mu_r \simeq 2Ld\gamma \,. \tag{6.2}$$

Therefore the free energy of the isotropic phase with a small amount of rigid rods is given by

$$\mathcal{F}_I^* = TVc \ln\left(\frac{f}{e}\right) + TV\frac{1-f}{N\nu}\ln\left(\frac{1-f}{e}\right) + Vc\mu_r \,. \tag{6.3}$$

Here we omitted the interaction between the rods. V is the volume of the system. In (6.3) the first two terms represent the translational entropy of the rods and coils.

The coils can also penetrate into the nematic phase. In order to write the free energy of the nematic phase with a small amount of coils we introduce the chemical potential of the coil in the nematic phase μ_c which includes both energetic and entropic contributions. Further on we consider the limit

$$\mu_c/T \to \infty \tag{6.4}$$

for arbitrary T. This means that the coils practically do not penetrate into the nematic phase.

The free energy of the nematic phase contains also a term connected with orientational ordering of rods. It can be estimated [140, 141] as $T\ln(4\pi/\Omega)$, where Ω is the characteristic fluctuation angle, $\Omega \simeq 2\pi(d/L)^2$. Thus the free energy is given by

$$\mathcal{F}_N^* = TVc\ln\left(\frac{f}{e}\right) + TV\frac{1-f}{N\nu}\ln\left(\frac{1-f}{e}\right) + 2TVc\ln\left(\frac{L}{d}\right) + V\frac{1-f}{N\nu}\mu_c. \tag{6.5}$$

The equilibrium between the nematic and isotropic phase can be found in the usual way by equating the chemical potentials and osmotic pressures in both phases.

$$\begin{aligned} \mu_I^* &= \mu_N^*; \quad \mu_{I,N}^* = \frac{1}{V}\frac{\partial \mathcal{F}_{I,N}^*}{\partial c} \\ P_I^* &= P_N^*; \quad P_{I,N}^* = \frac{1}{V}\left(c\,\frac{\partial \mathcal{F}_{I,N}^*}{\partial c} - \mathcal{F}_{I,N}^*\right). \end{aligned} \tag{6.6}$$

The solution of these equations is given by

$$f_N \simeq 1 - \kappa N\exp(-\mu_c/T) \simeq 1, \quad f_I \simeq \left(\frac{L}{d}\right)^2 \exp\left(-\frac{2L}{d}\left(\frac{w}{T}+s\right)\right) \ll 1. \tag{6.7}$$

This simple phenomenological model reflects the generic feature of the rod-coil mixtures to phase separate into almost pure components [120, 148]. The corresponding phase diagram is shown in Figure 6.2a.

6.3. Nematic – isotropic liquid phase coexistence: Effect of association

In this section we study the influence of association between rods and coils on the macrophase separation described above. We start from the free energy of association

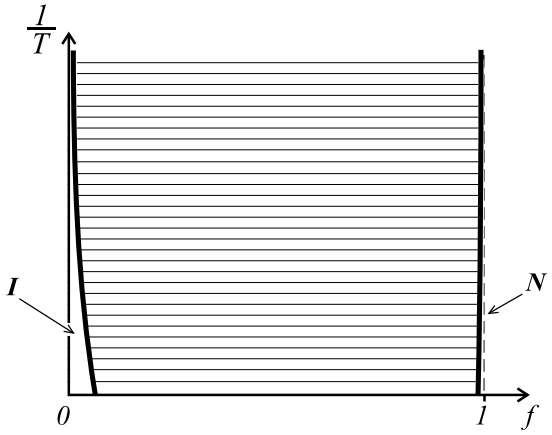

a

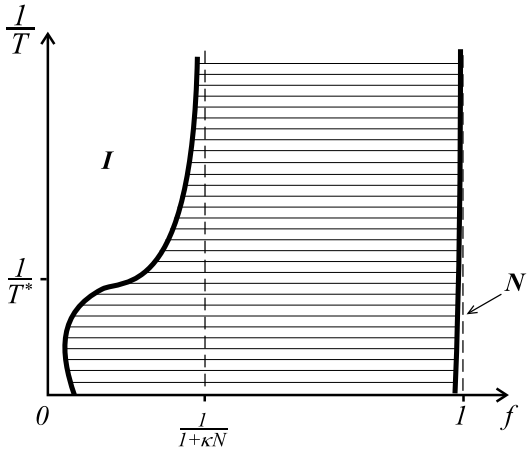

b

Figure 6.2: Macrophase equilibria in the associating rod-coil system: (a) no compatibility for small association energy; (b) enhanced compatibility in the $\epsilon/w > 2b/d$ case.

between rods and coils, $\mathcal{F}_{bond}$, assuming that they are ideal (without excluded volume). Let p denote the probability that an associating group of the rod has formed a bond with a flexible coil. The total number of bonds in the system is $VMcp$ and equals the number of *associated* coils. Therefore, the number of *free* coils in the system is $(V/N\nu)(1 - f - f\kappa pN)$, where $\kappa \equiv \nu/(\pi bd^2/4)$. The free energy of bonds can be expressed through the partition function Z_{bond} as [117, 149–151]

$$\mathcal{F}_{bond} = -T \ln Z_{bond} \,, \tag{6.8}$$

where

$$Z_{bond} = P_{comb} \left(\frac{v_b}{V}\right)^{VMcp} \exp\left(\frac{\epsilon\, VMcp}{T}\right) \tag{6.9}$$

and P_{comb} is the number of different ways to link rods and coils for a fixed probability p; v_b is the bond volume. If we denote the number of rods in the system as $\mathcal{N}_r = Vc$, and the number of coils as $\mathcal{N}_c = V(1 - f)/N\nu$, then the number of ways to choose $\mathcal{N}_r Mp$ coils for bond formation is the binomial coefficient

$$C_{\mathcal{N}_c}^{\mathcal{N}_r Mp} = \frac{\mathcal{N}_c!}{(\mathcal{N}_r Mp)!(\mathcal{N}_c - \mathcal{N}_r Mp)!} \,. \tag{6.10}$$

Moreover, there are

$$\frac{(\mathcal{N}_r M)!}{(\mathcal{N}_r M(1-p))!} \tag{6.11}$$

different ways to select $\mathcal{N}_r Mp$ bonds from $\mathcal{N}_r M$ associating groups. Therefore

$$P_{comb} = C_{\mathcal{N}_c}^{\mathcal{N}_r Mp} \frac{(\mathcal{N}_r M)!}{(\mathcal{N}_r M(1-p))!} \tag{6.12}$$

and the free energy of bonds is given by

$$\begin{aligned} \mathcal{F}_{bond} =& VMcp\left[T \ln\left(\frac{N\nu}{v_b}\right) - \epsilon\right] + TVcM\left[p \ln p + (1-p)\ln(1-p)\right] \\ &+ TV\frac{(1 - f - f\kappa Np)}{N\nu} \ln\left(\frac{1 - f - f\kappa Np}{e}\right) \\ &- TV\frac{(1-f)}{N\nu} \ln\left(\frac{1-f}{e}\right) . \end{aligned} \tag{6.13}$$

The free energy of the isotropic phase can be written as

$$\mathcal{F}_I = \mathcal{F}_I^* + \mathcal{F}_{bond} + \mathcal{F}_{el} \,, \tag{6.14}$$

where $\mathcal{F}_{el}$ is the elastic free energy of the side chains of the hairy-rod, which appears as soon as the density of association is high enough. We approximate it by [68, 72]

$$\mathcal{F}_{el} = \begin{cases} TVc\frac{3\kappa d^2}{32a^2}Mp^2\ln(\kappa Np), & p > \frac{1}{\kappa N} \\ 0, & \text{otherwise.} \end{cases} \tag{6.15}$$

Hence, the final expression for the free energy of the isotropic phase is given by (per volume of one rod $(\pi/4)Ld^2$)

$$\begin{aligned} \frac{F_I(f,p)}{T} =& f\frac{\mu_r}{T} + Mfp\left[\ln\left(\frac{N\nu}{v_b}\right) - \frac{\epsilon}{T}\right] + fM\left[p\ln p + (1-p)\ln(1-p)\right] \\ &+ f\ln\left(\frac{f}{e}\right) + M\frac{(1-f-f\kappa Np)}{N\kappa}\ln\left(\frac{1-f-f\kappa Np}{e}\right) \\ &+ f\frac{3\kappa d^2}{32a^2}Mp^2\ln(\kappa Np)\,H\left(p-\frac{1}{\kappa N}\right), \end{aligned} \tag{6.16}$$

where

$$H(x) = \begin{cases} 1, & x \geq 0 \\ 0, & x < 0 \end{cases}$$

is the Heavyside function. Similarly, the free energy of the nematic phase is

$$\begin{aligned} \frac{F_N(f,p)}{T} =& 2f\ln\left(\frac{L}{d}\right) + M\frac{1-f}{N\kappa}\frac{\mu_c}{T} + Mfp\left[\ln\left(\frac{N\nu}{v_b}\right) - \frac{\epsilon}{T}\right] \\ &+ fM\left[p\ln p + (1-p)\ln(1-p)\right] + f\ln\left(\frac{f}{e}\right) \\ &+ M\frac{(1-f-f\kappa Np)}{N\kappa}\ln\left(\frac{1-f-f\kappa Np}{e}\right). \end{aligned} \tag{6.17}$$

The probability of bonding in both phases can be found from the minimization of the corresponding free energies

$$\frac{\partial F_I}{\partial p} = 0; \quad \frac{\partial F_N}{\partial p} = 0 \tag{6.18}$$

and reads ($N^* \equiv N\nu/v_b$)

$$\begin{aligned} p = \frac{1}{2\kappa Nf}\Big[& 1 - f + \kappa Nf - N^*\exp(-\epsilon/T) \\ &- \sqrt{\left(1 - f + \kappa Nf - N^*\exp(-\epsilon/T)\right)^2 - 4\kappa Nf(1-f)}\ \Big] \end{aligned} \tag{6.19}$$

for the nematic phase and for the isotropic phase when $p < 1/\kappa N$. For $p > 1/\kappa N$ the probability of bonding in the isotropic phase satisfies

$$\ln\left[\frac{pN^*\mathrm{e}^{-\epsilon/T}}{(1-p)\,(1-f_I-f_I\kappa N p)}\right]+\frac{3\kappa d^2 p}{16a^2}\ln\left(\kappa N p\,\mathrm{e}\right)=0\,. \tag{6.20}$$

For a small volume fraction of rods, $f_I \ll 1$, it is approximately given by

$$p\simeq\frac{1}{1+N^*\mathrm{e}^{-\epsilon^*/T}},\quad \epsilon^*=\epsilon-\frac{3\kappa d^2 T}{32a^2}\,\frac{1}{1+N^*\mathrm{e}^{-\epsilon/T}}\ln\left(\frac{\kappa N}{1+N^*\mathrm{e}^{-\epsilon/T}}\right). \tag{6.21}$$

Phase equilibrium between the isotropic and nematic phase can be obtained in a standard way from the equilibrium equations[1]

$$\begin{aligned}\frac{\partial F_I}{\partial f_I} &= \frac{\partial F_N}{\partial f_N}\\ f_I\frac{\partial F_I}{\partial f_I}-F_I &= f_N\frac{\partial F_N}{\partial f_N}-F_N\,.\end{aligned} \tag{6.22}$$

using (6.16) and (6.17) together with (6.19) and (6.21).

At this point we have to consider two possible situations. The first one occurs if $\kappa N > 1$ so that both $p_I < 1/\kappa N$ and $p_I > 1/\kappa N$ are possible. The second one corresponds to $\kappa N < 1$ where the elastic tension of the associated coils is not important for any p.

Let us start from $\kappa N > 1$. When the probability of bonding in the isotropic phase $p_I < 1/\kappa N$, or equivalently $\epsilon/T < \ln((\kappa N-1)/N^*)$, expression (6.19) can be used giving the volume fraction of rods

$$\begin{aligned}f_N &\simeq 1,\\ f_I &\simeq \left(\frac{L}{d}\right)^2\exp\left(-\frac{\mu_r}{T}+\frac{M}{1+N^*\mathrm{e}^{-\epsilon/T}}\left(\frac{\epsilon}{T}-\ln N^*\right)\right)\ll 1\,.\end{aligned} \tag{6.23}$$

However, for lower temperatures p_I exceeds $1/\kappa N$ implying that the rods are densely grafted. Then the volume fraction of rods in the isotropic phase f_I satisfies the equation

$$\begin{aligned}\ln f_I - M p_I\ln\left(1-f_I-f_I\kappa N p_I\right)\simeq 2\ln\left(\frac{L}{d}\right)+\frac{M}{N\kappa}\\ -Mp_I\ln N^*-\frac{3\kappa d^2}{32a^2}Mp_I^2\ln(\kappa N)-\frac{2Ls}{d}+\frac{M}{T}\left(p_I\epsilon-\frac{2bw}{d}\right),\end{aligned} \tag{6.24}$$

[1]Expressions for the chemical potentials $\mu = \partial F/\partial f$ and partial pressures $P = f\,\partial F/\partial f - F$ for all the considered phases can be found in the Appendix 6.A.

where p_I has to be determined from (6.20). Obviously, $p_I \to 1$ if $T \to 0$ and therefore the last term in (6.24) becomes dominant. Depending on its sign two characteristic asymptotics can be distinguished

$$\begin{aligned} f_I &\to 0 \qquad \text{if} \quad \epsilon < \frac{2bw}{d}\,, \\ f_I &\to \frac{1}{1+N\kappa} \quad \text{if} \quad \epsilon > \frac{2bw}{d}\,. \end{aligned} \tag{6.25}$$

Thus for $\epsilon/w > 2b/d$ rods and coils become partially compatible. This fact has a clear physical meaning. A negative sign of $-\epsilon + (2bw/d)$ corresponds to a negative "total" energy (ϵ-part plus γ-part) due to the association of a coil to a rod, i.e. making it favorable to keep *all* coils bonded (for $T \to 0$, of course). In this case (6.24) gives the fraction of rods in the coil-rich phase and the region of the phase diagram below the temperature

$$T^* \simeq \frac{\epsilon - \frac{2bw}{d}}{\frac{2bs}{d} + \ln N^* + \frac{3\kappa d^2}{32a^2}\ln(\kappa N)} \tag{6.26}$$

reveals compatibility enhancement with the asymptotic value of the rod fraction $f_I \to 1/(1+\kappa N)$ for $T \to 0$. This situation is depicted in Figure 6.2b: a compatibility region occurs at low temperatures to the left of the stoichiometric point. For small association energies $\epsilon/w < 2b/d$ the situation is qualitatively identical to the one without association (see Figure 6.2a).

Now we turn to the case $\kappa N < 1$, when only low grafting densities are possible: p_I is always less than $1/\kappa N$. So the term responsible for the elastic stretching should be omitted according to approximation (6.16). This yields an equations for the isotropic phase density analogous to (6.24) but without the elastic $3\kappa d^2 \ln(\kappa N)/32a^2$ term. In the same way as above, the low temperature asymptotic $f_I \to 0$ appears for small association energy values corresponding to Figure 6.2a. In the opposite case of the high energies $\epsilon > 2bw/d$ (6.24) shows the tendency of f_I to increase approaching stoichiometric conditions $1/(1+\kappa N)$. However, it cannot be used in a quantitative manner because it is valid only for an isotropic phase with *small* amount of immersed rods (note that for $\kappa N < 1$ the value of $1/(1+\kappa N)$ is not small anymore).

6.4. Equilibria between nematic, isotropic and microphases for $\kappa N > 1$

As shown above, the association gives rise to a partial compatibility in the region of volume fractions up to the stoichiometric point $1/(1 + \kappa N)$. The existence of this region was proved above under the assumption that the phase is isotropic. However, due to attraction between hairy-rods immersed in a flexible chain melt, the formation of microdomained ordered structures may be expected.

In general, there are two mechanisms for attraction in hairy-rod systems. The first one arises from the inhomogeneous distribution of the free polymer coils [130] which creates some additional loss of entropy of the coils compared to the homogeneous melt [105] (see Appendix 6.B, where the interaction between two cylindrical micelles is analyzed). This mechanism ultimately results in the formation of microdomain lattice structures in the blend.

The second mechanism is connected to the incompatibility of rods and coils and is responsible for the selection between hexagonal and lamellar structures for certain values of the parameters. Furthermore, as in the case of the covalently bonded hairy-rods (see chapter 5 and [147]), we can distinguish two different hexagonal phases. In the first one, called H1, the "cylinders" contain only one rod per unit cell ($Q = 1$), Figure 6.3a. In the second one, called H2, the surface term becomes more important so that rods attract each other and the cylinders contain $Q > 1$ rods per unit cell, Figure 6.3b. On decreasing the temperature the cylinders transform to the lamellar phase.

Additionally we will prove that the tetragonal phase is unstable and is always suppressed by the hexagonal one.

6.4.1. Separation of the hexagonal phase H1

The attraction energy of cylinders resulting in the lattice formation of the hexagonal phases (H1, H2) is mainly due to the inhomogeneous distribution of the free polymer coils. Using the Random Phase Approximation it can be expressed in terms of the fluctuations of the monomeric density in the polymer matrix as [105, 130]

$$\frac{\Delta\mathcal{F}}{T} = \frac{\nu}{2N} \int \frac{|\Delta\phi_{free}(\mathbf{k})|^2}{g\left(\frac{a^2 N \mathbf{k}^2}{6}\right)} \frac{\mathrm{d}\mathbf{k}}{(2\pi)^3} \,. \tag{6.27}$$

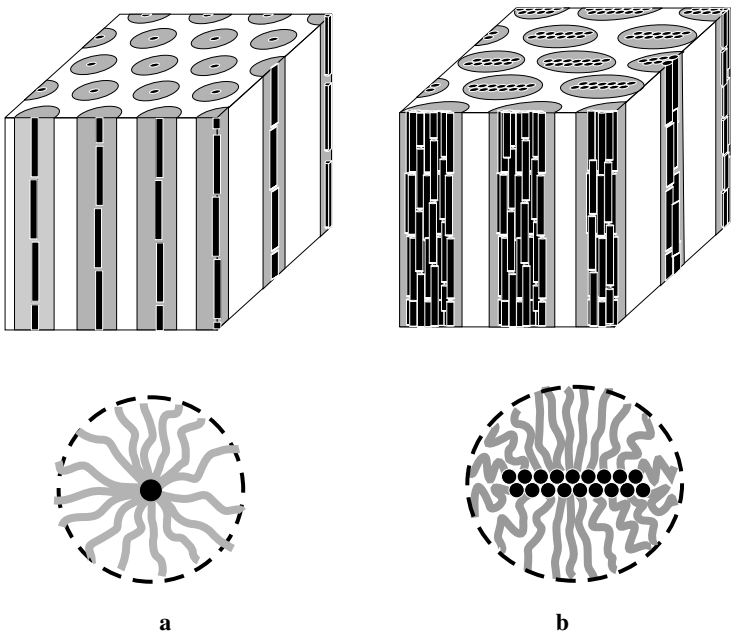

Figure 6.3: Possible hexagonal phases: (a) hexagonal H1; (b) hexagonal H2.

Here $\Delta\mathcal{F}$ is the free energy change relative to the homogeneous state and $g(u) = 2\left(u - 1 + \mathrm{e}^{-u}\right)/u^2$ is the Debye scattering function. $\Delta\phi_{free}(\mathbf{k})$ denotes the Fourier transform of the function $\phi_{free}(\mathbf{r}) - 1 \simeq -\phi_{assoc}(\mathbf{r})$, where ϕ_{free} and ϕ_{assoc} are the volume fractions of the free and associated coils defined at the mesoscopic level. Assuming that all coils obey Gaussian statistics and adopting the superposition approximation [130], where the overall density of the associated coils ϕ_{assoc} is a simple sum of corona's densities of the individual cylinders fixed in the vertices of the lattice, we arrive at the interaction energy (per cylinder of unit length)

$$\frac{\mathcal{U}_H(Q)}{T} = \frac{N\nu(Qp)^2}{2b^2}\left[\frac{2}{\sqrt{3}\,\ell^2}\sum_{\{\mathbf{b}_r\}}\frac{h^2(\frac{a^2N\mathbf{k}^2}{6})}{g(\frac{a^2N\mathbf{k}^2}{6})} - \frac{1}{4\pi^2}\int \mathrm{d}\mathbf{k}\frac{h^2(\frac{a^2N\mathbf{k}^2}{6})}{g(\frac{a^2N\mathbf{k}^2}{6})}\right], \qquad (6.28)$$

where ℓ is the period of the structure, $\{\mathbf{b}_r\}$ are the vectors of the reciprocal lattice, and $h(u) = \left(1 - \mathrm{e}^{-u}\right)/u$.

The first term in (6.28) arises directly from (6.27), whereas the second one is the energy of the lattice with infinite period, which is used as a reference point. The period of the structure can be easily related to the volume fraction of rods as

$$\ell^2 = \frac{1}{2\sqrt{3}} \frac{\pi d^2 Q}{f} . \tag{6.29}$$

After calculation of the sum and integral in (6.28), Appendix 6.C, we find the interaction energy and renormalize it per volume $(\pi/4)Ld^2$

$$\frac{U_H(Q)}{T} = -\frac{3}{32} \frac{\kappa M Q p^2 f d^2}{a^2} \left[3.457 + \ln\left(\frac{a^2 N f}{Q d^2} \right) \right] . \tag{6.30}$$

Thus the free energy of the H1 phase ($Q = 1$) is given by

$$\begin{aligned} \frac{F_{H1}}{T} =& 2fLd\frac{\gamma}{T} - Mfp\left[\frac{\epsilon}{T} - \ln N^* \right] + fM\left[p\ln p + (1-p)\ln(1-p) \right] \\ &+ 2f\ln\left(\frac{L}{d} \right) + M\frac{(1-f-f\kappa Np)}{N\kappa} \ln\left(\frac{1-f-f\kappa Np}{e} \right) \\ &+ f\frac{3\kappa d^2}{32a^2} Mp^2 \ln(\kappa Np) - \frac{3}{32} \frac{\kappa M p^2 f d^2}{a^2} \left[3.457 + \ln\left(\frac{a^2 N f}{d^2} \right) \right] . \end{aligned} \tag{6.31}$$

Here we approximated the loss of orientational energy of a rod by the term $2Tf\ln(L/d)$ and omitted the loss of its translational entropy because it is relatively small. Phase equilibrium between the isotropic phase and the H1 phase can be found from the equilibrium equations

$$\begin{aligned} \frac{\partial F_I}{\partial f_I} = \frac{\partial F_{H1}}{\partial f_{H1}}, \qquad & \frac{\partial F_I}{\partial p_I} = \frac{\partial F_{H1}}{\partial p_{H1}} = 0 \\ f_I \frac{\partial F_I}{\partial f_I} - F_I \quad = \quad & f_{H1} \frac{\partial F_{H1}}{\partial f_{H1}} - F_{H1} . \end{aligned} \tag{6.32}$$

The probability of bonding and the binodal lines are

$$\begin{aligned} & p_I \simeq p_{H1} \simeq 1, \\ & f_{H1}^{(1)} \simeq \frac{3}{16} \frac{d^2}{a^2 N}, \\ & f_I \simeq \left(\frac{L}{d} \right)^2 \exp\left(-\frac{3}{16} \frac{d^2 \kappa M}{a^2} \right) \simeq 0 . \end{aligned} \tag{6.33}$$

Similarly the phase equilibrium between the nematic and the H1 phase follows from equations

$$\begin{aligned} \frac{\partial F_N}{\partial f_N} = \frac{\partial F_{H1}}{\partial f_{H1}}, \qquad & \frac{\partial F_N}{\partial p_N} = \frac{\partial F_{H1}}{\partial p_{H1}} = 0, \\ f_N \frac{\partial F_N}{\partial f_N} - F_N \quad = \quad & f_{H1} \frac{\partial F_{H1}}{\partial f_{H1}} - F_{H1} \,. \end{aligned} \tag{6.34}$$

Their solution is given by

$$\begin{aligned} & p_N \simeq 0, \quad p_{H1} \simeq 1, \\ & f_N \simeq 1, \\ & f_{H1}^{(2)} \simeq \frac{1}{1+\kappa N} \left[1 - \exp\left(-\frac{\epsilon}{T} + 2bd\frac{\gamma}{T} + \ln N^* + \frac{3\kappa d^2}{32a^2} \ln(\kappa N) \right) \right] . \end{aligned} \tag{6.35}$$

The triple point T_0, where isotropic, nematic and H1 phases coexist, can be obtained from the intersection of the curves $f_{H1}^{(1)}(T)$ and $f_{H1}^{(2)}(T)$ and reads

$$\frac{\epsilon}{T_0} = \frac{1}{1 - \frac{2bw}{\epsilon d}} \left(\frac{2bs}{d} + \ln N^* + \frac{3\kappa d^2}{32a^2} \ln(\kappa N) \right) , \tag{6.36}$$

where the probability of bonding $p_0 \simeq 1$. Thus the hexagonal H1 phase is stable for $f_{H1}^{(1)} < f < f_{H1}^{(2)}$ below T_0; for $f_I < f < f_{H1}^{(1)}$ the system separates into the isotropic and the H1 phase and for $f_{H1}^{(1)} < f < f_N$ it separates into the H1 and the nematic phase (see Figure 6.4).

It is also interesting to note that at the triple point the period of the hexagonal structure is $\ell = \left(8\pi/(3\sqrt{3})\right)^{1/2} a\sqrt{N} \simeq 2a\sqrt{N}$ so that the system has the structure of almost close-packed cylinders. As we have shown in Appendix 6.B, the two micelles interaction energy reveals minimum at the distance $r_{12} \simeq 3.3a\sqrt{N}$. Although it seems natural to assume that the period ℓ of the appearing lattice is equal to r_{12}, in reality it is much smaller $\ell \simeq 2a\sqrt{N}$. This becomes possible because repulsion between closest neighbors is compensated by attraction between more distant micelles.

Apparently, a question about the possible existence of a tetragonal (2D square lattice) phase arises at this point. It would correspond to a lower density of rods and might possibly appear at *higher* temperatures $T > T_0$. In the framework of the method employed, the only difference between the H1 and the tetragonal phase is the interaction energy corresponding to the different lattices. The latter, equation

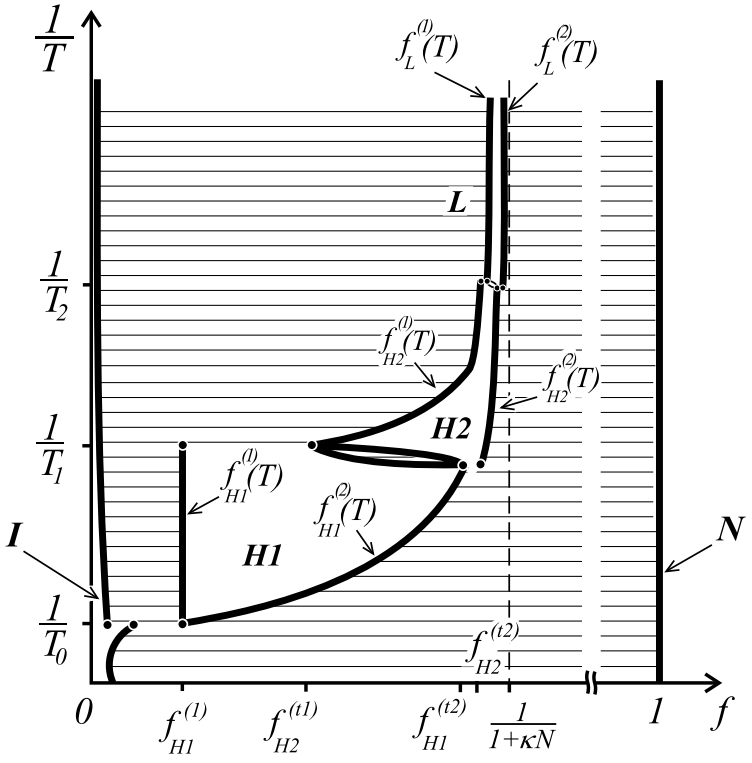

Figure 6.4: Complete phase diagram in the case $\kappa N > 1$

(6.115), is calculated using the same method as explained above (6.27) in Appendix 6.C. It can be shown that the critical point T_T, at which the tetragonal structure would appear, lies below the point T_0 for any values of the model's parameters: $T_T < T_0$. This implies that the tetragonal phase is always suppressed by the hexagonal phase.

6.4.2. Separation of the hexagonal phase H2

Decreasing the temperature T, we effectively increase the repulsion between the rods and coils due to the surface tension (see e.g. the first term in (6.31)). This results in the tendency of rods to adopt a packing with smaller total area of contact with coils. It makes the H2 phase more favorable comparing to the H1, but at the same time leads to an increase in the elastic energy of the side chains (see Figure 6.3). The competition between these two factors results in the H1–H2 transition.

Let us follow along the binodal line $f_{H1}^{(1)}(T)$ with the temperature going down (Figure 6.4). At a certain moment phase H1 becomes unstable compared to separation into the isotropic and the hexagonal H2 phase. The corresponding triple point can be obtained from the set of equations

$$\frac{\partial F_I}{\partial f_I} = \frac{\partial F_{H1}}{\partial f_{H1}} = \frac{\partial F_{H2}}{\partial f_{H2}}\,, \qquad \frac{\partial F_I}{\partial p_I} = \frac{\partial F_{H1}}{\partial p_{H1}} = \frac{\partial F_{H2}}{\partial p_{H2}} = 0\,,$$
$$f_I \frac{\partial F_I}{\partial f_I} - F_I = f_{H1} \frac{\partial F_{H1}}{\partial f_{H1}} - F_{H1} = f_{H2} \frac{\partial F_{H2}}{\partial f_{H2}} - F_{H2}\,. \tag{6.37}$$

In order to construct the free energy F_{H2} of the H2 phase one has to modify the surface tension and the elastic energy terms in (6.31).

Assuming that coils cannot penetrate inside, the core of the cylindrical micelle the core adopts a double layer structure of closely packed rods, as depicted in Figure 6.3b, with a surface per unit length along the cylinder $Qd + 2d$ valid for $Q > 2$ (see also 5). For $Q < \sqrt{N}$ the cylinders still have an approximately circular cross section so that

the approximation (6.15) with renormalized grafting density can be used. Thus

$$\begin{aligned}\frac{F_{H2}}{T} =& fLd\frac{\gamma}{T}\left(1+\frac{2}{Q}\right)+Mfp\left[\ln N^{*}-\frac{\epsilon}{T}\right]\\ &+fM\left[p\ln p+(1-p)\ln(1-p)\right]+2f\ln\left(\frac{L}{d}\right)\\ &+M\frac{(1-f-f\kappa Np)}{\kappa N}\ln\left(\frac{1-f-f\kappa Np}{e}\right)\\ &+f\frac{3d^{2}\kappa Q}{32a^{2}}Mp^{2}\ln(\kappa Np)\\ &-\frac{3}{32}\frac{\kappa MQp^{2}fd^{2}}{a^{2}}\left[3.457+\ln\left(\frac{a^{2}Nf}{Qd^{2}}\right)\right]. \end{aligned} \tag{6.38}$$

The number of rods per unit cell Q follows from the minimum condition $\partial F_{H2}/\partial Q = 0$,

$$Q \simeq \sqrt{\frac{64ba^{2}}{3\kappa p^{2}d\ln(\kappa N)}\frac{\gamma}{T}}\,. \tag{6.39}$$

In derivation of (6.39) we used the fact that Q is mainly determined by the interplay between the surface term and the elastic energy of the grafted coils, omitting the relatively small "lattice" term (the last one in (6.38)).

Hence, the solution of (6.37) is given by

$$\begin{aligned} &p_{I} \simeq p_{H1} \simeq p_{H2} \simeq 1,\\ &Q_{1} \simeq 2+\sqrt{2}, \quad f_{I} \simeq 0,\\ &f_{H1}^{(t1)} \simeq \frac{3}{16}\frac{d^{2}}{a^{2}N}, \quad f_{H2}^{(t1)} \simeq \frac{3}{16}\frac{Q_{1}d^{2}}{a^{2}N}, \end{aligned} \tag{6.40}$$

and the critical temperature reads

$$\frac{w}{T_{1}} \simeq -s+\frac{3\kappa d^{3}Q_{1}^{2}}{64ba^{2}}\ln(\kappa N)\,. \tag{6.41}$$

Similarly the binodal line $f_{H2}^{(2)}(T)$ finishes at the triple point, which can be found from the system of equations

$$\begin{aligned} &\frac{\partial F_{N}}{\partial f_{N}}=\frac{\partial F_{H1}}{\partial f_{H1}}=\frac{\partial F_{H2}}{\partial f_{H2}}, \quad \frac{\partial F_{N}}{\partial p_{N}}=\frac{\partial F_{H1}}{\partial p_{H1}}=\frac{\partial F_{H2}}{\partial p_{H2}}=0,\\ &f_{N}\frac{\partial F_{N}}{\partial f_{N}}-F_{N}=f_{H1}\frac{\partial F_{H1}}{\partial f_{H1}}-F_{H1}=f_{H2}\frac{\partial F_{H2}}{\partial f_{H2}}-F_{H2} \end{aligned} \tag{6.42}$$

and is characterized by

$$\begin{aligned}
p_N &\simeq 0, \quad p_{H1} \simeq p_{H2} \simeq 1, \\
Q_1^{'} &\simeq Q_1 \simeq 2 + \sqrt{2}, \quad f_N \simeq 1, \\
f_{H1}^{(t2)} &\simeq \frac{1}{1+\kappa N}\left[1 - \exp\left(-\frac{\epsilon}{T_1} + \frac{2bd\gamma}{T_1} + \ln N^* + \frac{3d^2\kappa}{32a^2}\ln(\kappa N)\right)\right], \\
f_{H2}^{(t2)} &\simeq \frac{1}{1+\kappa N}\left[1 - \exp\left(-\frac{\epsilon}{T_1} + \frac{bd\gamma}{T_1}\left(1 + \frac{2}{Q_1}\right)\right.\right. \\
&\quad \left.\left. + \ln N^* + \frac{3d^2\kappa Q_1}{32a^2}\ln(\kappa N)\right)\right]. \qquad (6.43)
\end{aligned}$$

In a first approximation the corresponding critical temperature coincides with the critical temperature (6.41). Note, the small difference between these critical temperatures, which we do not consider here, results in a small area of phase coexistence between H1 and H2 (see Figure 6.4). Also the triple points $f_{H1}^{(t2)}$ and $f_{H2}^{(t2)}$ are exponentially close to each other. Using (6.40) and (6.43) we conclude that the average number of molecules per micelle of length L is $Q_1 = 2 + \sqrt{2} \simeq 3.4$ when H2 first appears. Hence, the cylindrical domain has 3-4 rods in its cross section. This small number is consistent with the approximation used concerning the almost circular cross section.

The phase equilibrium between the isotropic and the hexagonal H2 phase is determined from the set of equations

$$\begin{aligned}
&\frac{\partial F_I}{\partial f_I} = \frac{\partial F_{H2}}{\partial f_{H2}}, \quad \frac{\partial F_I}{\partial p_I} = \frac{\partial F_{H2}}{\partial p_{H2}} = 0, \\
&f_I \frac{\partial F_I}{\partial f_I} - F_I = f_{H2}\frac{\partial F_{H2}}{\partial f_{H2}} - F_{H2}, \qquad (6.44)
\end{aligned}$$

which has different asymptotic solutions near the triple point and far away from it. A simple expansion in the vicinity of the $f_{H2}^{(t1)}$ point gives the binodal line in the form

$$f_{H2}^{(1)}(T) \simeq \frac{3}{16}\frac{d^2}{a^2 N} Q(T), \qquad (6.45)$$

whereas for $1 \ll Q < \sqrt{N}$ the solution of (6.44) reads

$$\begin{aligned}
&p_I \simeq p_{H2} \simeq 1, \\
&f_I \simeq 0, \\
&f_{H2}^{(1)} \simeq \frac{1}{1+\kappa N}\left[1 - \exp\left(-\frac{3}{16}\frac{d^2}{a^2 N} Q(T)\right)\right]. \qquad (6.46)
\end{aligned}$$

Here $Q(T)$ is given by (6.39) and is temperature dependent.

Similar equilibrium conditions have to be applied to the nematic-H2 coexistence yielding the result

$$\begin{aligned} p_N &\simeq 0, \quad p_{H2} \simeq 1, \\ f_N &\simeq 1, \\ f_{H2}^{(2)} &\simeq \frac{1}{1+\kappa N}\left[1 - \exp\left(-\frac{\epsilon}{T} + \frac{bd\gamma}{T}\left(1 + \frac{2}{Q(T)}\right)\right.\right. \\ &\quad \left.\left. + \ln N^* + \frac{3d^2\kappa Q(T)}{32a^2}\ln(\kappa N)\right)\right]. \end{aligned} \tag{6.47}$$

The results obtained for the binodal lines and the triple points are summarized in Figure 6.4.

With further decrease of the temperature the number of rods in the cross section Q increases going beyond the limit $Q < \sqrt{N}$. The core of the cylinders containing the rods becomes considerably elongated and the approximation (6.15) fails. It this case a planar rather than a circular cylindrical shape of the core should be taken as a reference state, reflecting the very high values of $Q \sim N$ in the vicinity of the hexagonal H2 to lamellar phase transition. We will address this in the next subsection.

6.4.3. Separation of the lamellar phase

Following the same procedure as before we proceed with the derivation of the free energy of the lamellar phase. Compared to the hexagonal phases, a number of terms has to be modified. Here we start from **the interaction between lamellae**.

Apparently, the total energy of the lamellae's interaction is a sum of all the nearest neighbor interaction energies. We briefly outline the calculation scheme here (see [130, 152] for details). Let us consider first a *single* lamella immersed in a melt of flexible chains. The free energy per unit area of the lamella consists of the free energy of the attached $\Delta F^{(a)}$ and free $\Delta F^{(f)}$ coils.

$$\Delta F = \Delta F^{(a)} + \Delta F^{(f)}. \tag{6.48}$$

The last one is given by

$$\Delta F^{(f)} = \frac{a^2 T}{24\nu}\int \frac{(\nabla\phi_f)^2}{\phi_f}\,\mathrm{d}z,$$

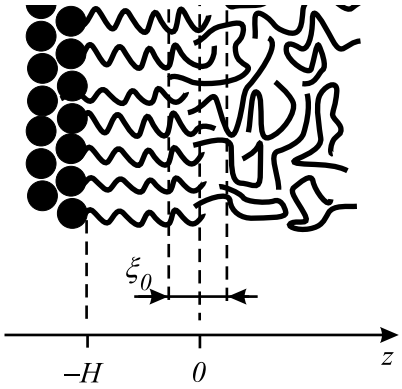

a

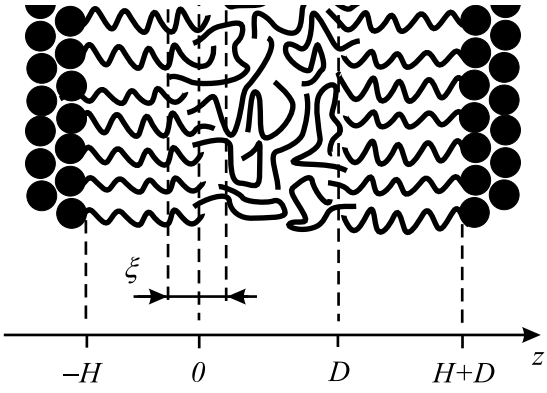

b

Figure 6.5: (a) Single lamella and its surrounding. (b) Two neighboring lamellae.

where $\phi_f(z)$ is the volume fraction of the free coils and the z axis points perpendicular to the lamella's plane (see Figure 6.5a). The $\Delta F^{(a)}$ term consists of two parts

$$\Delta F^{(a)} = \frac{a^2 T}{24\nu} \int \frac{(\nabla \phi_a)^2}{\phi_a} \mathrm{d}z - \frac{T}{\nu} \int_0^\infty u(z) \left[\phi_a(z) - \phi_a^{(box)} \right] \mathrm{d}z \,, \tag{6.49}$$

where the second term takes into account the additional energy of the attached coils' elastic elongation compared to its minimum value, corresponding to a box-like density distribution $\phi_a^{(box)}(z)$. Here

$$u(z) = \frac{3\pi^2}{8} \frac{(z+H)^2}{N^2 a^2} \tag{6.50}$$

is the parabolic molecular field responsible for the stretching of the attached coils [131, 152] and H is the width of the corona consisting of the attached coils. The deviation from the box-like distribution creates an interpenetration area ξ_0 (see Figure 6.5a), which in its turn is determined from the minimization of (6.48) with a trial function of the form

$$\phi_a = 1 - \phi_f = \frac{1}{2} \left(1 - \tanh \frac{z}{\xi_0} \right) . \tag{6.51}$$

After the minimization ξ_0 is obtained

$$\xi_0 = \left(\frac{4}{3\pi^4} \frac{N^2 a^4}{H} \right)^{1/3} \tag{6.52}$$

as well as the free energy of the lamella

$$\Delta F_\infty = \min_{\xi_0} \Delta F = \frac{\pi T}{8\nu} \left(\frac{3\pi a^2 H}{4N^2} \right)^{1/3} . \tag{6.53}$$

Using the same approach, the interaction between two lamellae can be considered too. For this purpose we examine two planar micelles put on a distance D from each other as depicted in Figure 6.5b. Their interaction energy (per unit area) reads

$$\mathcal{U}(D) = \Delta F(D) - 2F_\infty \,, \tag{6.54}$$

where similarly to the previously explained case

$$\Delta F(D) = \min_{\xi} \left[2\Delta F^{(a)}(\xi) + \Delta F^{(f)}(\xi, D) \right] . \tag{6.55}$$

Of course, ξ depends now on D; also an appropriate trial function has to be taken for the minimization procedure

$$\phi_f(z) = \frac{1}{2}\left[\tanh\frac{z}{\xi} + \tanh\frac{D-z}{\xi}\right]. \tag{6.56}$$

Without going into details of the calculation we present the final result (see also [130, 152])

$$\begin{aligned} \xi_{min}(D) &\simeq \xi + \frac{4}{9}D\,, \\ \xi &= \left(\frac{2}{3\pi^4}\,\frac{N^2a^4}{H}\right)^{1/3} \end{aligned} \tag{6.57}$$

and

$$\Delta F(D) \simeq \frac{a^2T}{8\nu\xi} + \frac{a^2TD}{18\nu\xi^2}\,. \tag{6.58}$$

The variables D and H can be easily related to the volume fraction of rods f and other characteristic quantities of the system as

$$\begin{aligned} D &= \frac{\pi d}{2}\,\frac{f^* - f}{f^{*2}}\,, \\ H &= \frac{\pi d}{4}\kappa N p\,, \end{aligned} \tag{6.59}$$

where $f^* = 1/(1+\kappa N p)$ is the volume fraction of rods if all coils in the system are attached.

Hence, using equations (6.54) and (6.57)–(6.59), and renormalizing the energy as per volume $\pi d^2 L/4$, the interaction energy is obtained

$$\frac{U_L(f)}{T} = -0.227 f^* M\left(\frac{pa^2}{\kappa^2 d^2 N}\right)^{1/3} + 1.312 M\left(\frac{p^2d^2}{\kappa a^2 N^2}\right)^{1/3}\frac{f^* - f}{f^*}\,. \tag{6.60}$$

The expression for the **elastic free energy** of the coils attached to a planar surface is trivial considering that the stretching free energy of one coil is [1, 2] $F_1 = 3TH^2/(2Na^2)$.

So far the free energy of the lamellar phase is obtained in the form

$$\begin{aligned}\frac{F_L}{T} &= fLd\frac{\gamma}{T} + Mfp\left[\ln N^* - \frac{\epsilon}{T}\right] + fM\left[p\ln p + (1-p)\ln(1-p)\right] \\ &\quad +2f\ln\left(\frac{L}{d}\right) + M\frac{(1-f-f\kappa Np)}{\kappa N}\ln\left(\frac{H}{\xi}\,\frac{1-f-f\kappa Np}{e}\right) \\ &\quad +f\frac{3\pi^2d^2\kappa^2}{32a^2}NMp^3 + \frac{U_L(f)}{T}\,. \end{aligned} \tag{6.61}$$

where ξ according to (6.57) and (6.59) is given by

$$\xi = \frac{2a}{\pi}\left(\frac{aN}{3\pi^2\kappa pd}\right)^{1/3}\,. \tag{6.62}$$

Here we have taken into account that any given free coil is confined in a space of width 2ξ between a pair of two successive lamellae separated by a distance $2H$. Therefore, the free coils additionally loose some translational entropy compared to the hexagonal and isotropic phase.

The phase equilibrium between the isotropic and the lamellar phase can be described on the basis of the equations

$$\begin{aligned}&\frac{\partial F_I}{\partial f_I} = \frac{\partial F_L}{\partial f_L}, \quad \frac{\partial F_I}{\partial p_I} = \frac{\partial F_L}{\partial p_L} = 0, \\ &f_I\frac{\partial F_I}{\partial f_I} - F_I = f_L\frac{\partial F_L}{\partial f_L} - F_L \end{aligned} \tag{6.63}$$

and the probability of bonding and the binodals are given by

$$\begin{aligned}&p_I \simeq p_L \simeq 1, \\ &f_I \simeq 0, \\ &f_L^{(1)} \simeq \frac{1}{1+\kappa N}\left[1 - \frac{\xi}{H}\exp\left(-1.312\left(\frac{\kappa^2d^2N}{a^2}\right)^{1/3}\right)\right]. \end{aligned} \tag{6.64}$$

Similarly the equilibrium between the nematic and the lamellar phase must fulfill the set of equations

$$\begin{aligned}&\frac{\partial F_N}{\partial f_N} = \frac{\partial F_L}{\partial f_L}, \quad \frac{\partial F_N}{\partial p_N} = \frac{\partial F_L}{\partial p_L} = 0, \\ &f_N\frac{\partial F_N}{\partial f_N} - F_N = f_L\frac{\partial F_L}{\partial f_L} - F_L\,, \end{aligned} \tag{6.65}$$

from which the corresponding probabilities and binodals are obtained

$$\begin{aligned} &p_N \simeq 0, \quad p_L \simeq 1, \\ &f_N \simeq 1, \\ &f_L^{(2)} \simeq \frac{1}{1+\kappa N}\left[1 - \exp\left(\frac{-\epsilon + bd\gamma}{T} + \ln N^* + \frac{3\pi^2 d^2 \kappa^2 N}{32a^2}\right)\right]. \end{aligned} \tag{6.66}$$

Now we would like to address the question about the hexagonal H2 to lamellar phase transition. As it was pointed out before, in the vicinity of the transition the core of the H2-phase cylinders have a considerably non-circular shape (Figure 6.3b). Therefore, the calculation of the elastic energy and the interaction between this kind of cylinders becomes a nontrivial task. However, taking into account the highly elongated shape of the cores of the H2-cylinders near the transition, the elastic free energy of the side chains can be approximated as that of the corresponding planar lamella plus some edge correction following the method developed in [144]. Here we do not go into details of the calculation referring the reader to the previous chapter, where the following expression (see (5.17)) has been obtained for this edge correction

$$\widetilde{F} \simeq -\frac{3fT}{Q}\,\frac{\nu H^2 M p^2}{a^2 b d^2}\,. \tag{6.67}$$

Hence, the elastic free energy of the H2 phase *near* the H2 to lamellar phase transition is approximated by

$$\frac{F'^{(el)}_{H2}}{T} \simeq \frac{3\pi^2 d^2 \kappa}{32a^2} f N M p^3 - 3\left(\frac{\pi\kappa}{4}\right)^3 \frac{d^2 N^2 M p^4}{a^2}\,\frac{f}{Q}\,. \tag{6.68}$$

In the very vicinity of the transition between H2 cylinders and lamellae the interaction energy in the H2-phase can be approximated by the corresponding one for the lamella (6.60), yielding

$$\begin{aligned} \frac{F'_{H2}}{T} =& fLd\frac{\gamma}{T}\left(1 + \frac{2}{Q}\right) + Mfp\left[\ln N^* - \frac{\epsilon}{T}\right] \\ &+ fM\left[p\ln p + (1-p)\ln(1-p)\right] + 2f\ln\left(\frac{L}{d}\right) \\ &+ M\frac{(1 - f - f\kappa N p)}{\kappa N}\ln\left(\frac{1 - f - f\kappa N p}{e}\right) + \frac{F'^{(el)}_{H2}}{T} + \frac{U_L}{T}\,. \end{aligned} \tag{6.69}$$

Comparing (6.69) to (6.61) one concludes that the H2–Lam transition is completely determined by the interplay between the elastic and the surface tension term. The quantitative result follows from the equilibrium conditions

$$\frac{\partial F_L}{\partial f_L} = \frac{\partial F'_{H2}}{\partial f_{H2}}, \quad \frac{\partial F_L}{\partial p_L} = \frac{\partial F'_{H2}}{\partial p_{H2}} = 0,$$
$$f_N \frac{\partial F_L}{\partial f_L} - F_L = f_{H2} \frac{\partial F'_{H2}}{\partial f_{H2}} - F'_{H2}\,. \tag{6.70}$$

The area of the lamellar-H2 phase coexistence is very narrow, like it was in the H1-H2 case, implying that the corresponding triple points (H2-Lam-Nem and H2-Lam-Iso; see Figure 6.4) are exponentially close to each other and characterized by the temperature T_2

$$\frac{w}{T_2} \simeq \frac{3}{2}\left(\frac{\pi\kappa d}{4}\right)^3 \frac{N^2}{ba^2} - s\,. \tag{6.71}$$

Note that the number of rods per cylinder in the H2-phase dropped out from the result (6.71) *without* minimization. This fact is connected to the approximation (6.68), which in a sense can be viewed as an expansion in the small parameter $1/Q$. So, to obtain the number of rods Q_2 at the H2-Lam transition consistently one has to extend the approximation (6.68). However, Q_2 can be also estimated from (6.68) when the edge correction becomes of the order of the main term

$$Q_2 \sim \kappa N\,. \tag{6.72}$$

6.4.4. Possible phase sequences

In the previous subsections a complete phase diagram was described for the highly grafted supramolecular hairy-rod system. However, an implicit assumption about the presence of all the three microphases was used. Certainly, depending on the values of the model's parameters (mainly the ratio ϵ/w) other sequences of microphases are possible.

The prediction about the realization of a particular phase diagram can be made from a comparison of the temperatures where the microphases first appear. For instance, the simple hexagonal phase H1 is present if the temperature T_0 given by (6.36) is higher than T_1 (6.41), where a transition to H2 occurs. This leads to the conclusion that the phase diagram has the form shown in Figure 6.4 only if

$$\frac{\epsilon d}{2bw} > 1 + \frac{\frac{3\kappa d^2}{32a^2}\ln(\kappa N) + \ln N^* + \frac{2bs}{d}}{\frac{3\kappa d^2}{32a^2}(6+4\sqrt{2})\ln(\kappa N) - \frac{2bs}{d}}\,. \tag{6.73}$$

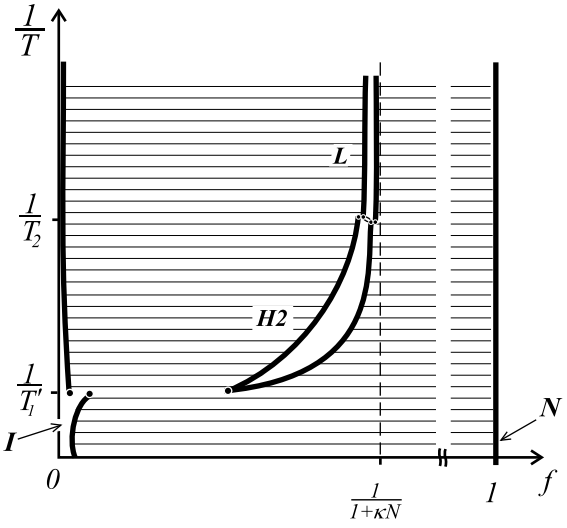

a

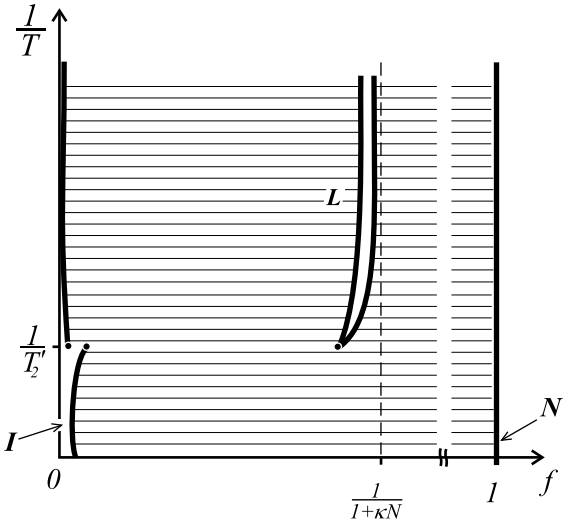

b

Figure 6.6: Two more possible phase diagrams in the $\kappa N > 1$ case (see also Figure 6.4 and eqs (6.73), (6.74))

In the absence of both hexagonal phases the lamellar phase would appear at the point determined as the intersection of the curves $f_L^{(1)}(T)$ and $f_L^{(2)}(T)$(equations (6.64) and (6.66)). This point is lower than T_2 (6.24) if the following condition is fulfilled

$$1 < \frac{\epsilon d}{bw} < 1 + \frac{4b}{\pi d \kappa N}\,. \tag{6.74}$$

Thus, only nematic, isotropic and lamellar phases coexist in this case and the corresponding diagram is shown in Figure 6.6b.

Finally, for values of ϵ/w lying in between that of the regimes (6.73) and (6.74) only H2 and lamellar structures are stable as depicted in Figure 6.6a.

6.5. Phase equilibria for $\kappa N < 1$

In this section we consider the phase behavior of the same rod-coil system as before, but for small values of the parameter $\kappa N < 1$. As explained above, this implies a low grafting density of coils attached to a rod even for conversion $p = 1$. A direct consequence in the framework of the presented model is the absence of the elastic stretching term in the free energies of all phases considered. In fact, the free energies of the isotropic liquid and both hexagonal phases can be borrowed from the previous calculation, equations (6.16), (6.31) and (6.38), keeping in mind that the term responsible for the stretching of coils has to be omitted everywhere.

However, the lamellar phase needs some additional attention. The expression for the lattice free energy (6.60) was obtained by a method [130, 152] assuming high surface density of the attached coils. Definitely, for $\kappa N < 1$ this is not the case anymore. Therefore, another method, based on (6.27), should be adopted for this purpose. Using the same arguments as for the hexagonal phase (see Appendix 6.C) one arrives at the expression for the lattice energy of the lamellar structure:

$$\frac{U_L'(f)}{T} \simeq \frac{\pi^2}{128}\,\frac{M\kappa p^2 d^2}{a^2} + \frac{Mf\kappa p^2 d\sqrt{N}}{8a}\left[-1.728 + \frac{af\sqrt{N}}{d}\right]. \tag{6.75}$$

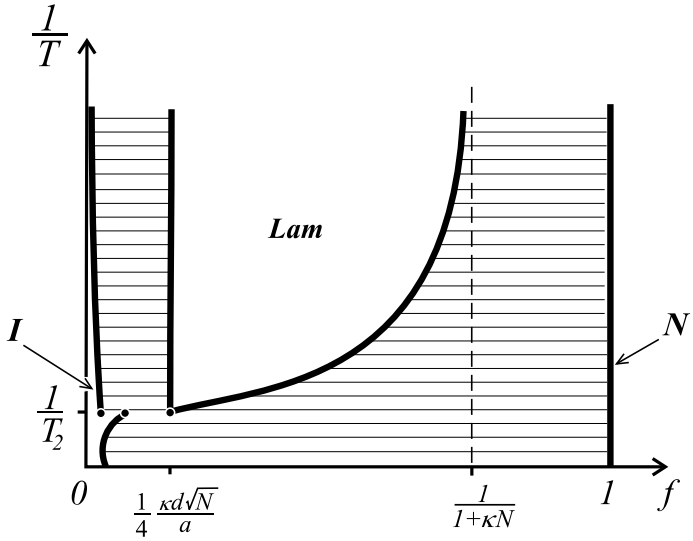

Figure 6.7: Phase diagram of the system for $\kappa N < 1$.

Therefore, the total free energy of the lamellar phase (per volume of a rod) reads

$$\begin{aligned}\frac{F'_L}{T} =& fLd\frac{\gamma}{T} + Mfp\left[\ln N^* - \frac{\epsilon}{T}\right] \\ &+ fM\left[p\ln p + (1-p)\ln(1-p)\right] + 2f\ln\left(\frac{L}{d}\right) \\ &+ M\frac{(1-f-f\kappa Np)}{\kappa N}\ln\left(\frac{H}{\xi}\,\frac{1-f-f\kappa Np}{e}\right) + \frac{U'_L(f)}{T}\,. \end{aligned} \tag{6.76}$$

Further analysis shows that, in contrast to the previously considered high grafting density situation, only the lamellar structure accompanied by nematic and isotropic liquid is present in the phase diagram Figure 6.7. It first appears at the temperature

$$\frac{1}{T_2} = \frac{\ln N^* + bs/d}{\epsilon - bw/d} \tag{6.77}$$

and takes a prominent place in the phase diagram totally suppressing both hexagonal phases.

This fact is also supported by our physical expectations. The actual selection between H1, H2 and Lam phases in the case $\kappa N > 1$ was performed by an interplay

between the surface tension γ-term and the elastic stretching of the side chains. At relatively high temperatures the surface tension was small and therefore the system adopted the hexagonal structure characterized by lower elastic energy. However, as the temperature is decreased, the surface tension starts to play the dominant role and the system transforms to the lamellar phase where the total contact area between rods and coils is much smaller. In the current case of $\kappa N < 1$ the elastic energy is not important at all. This implies the dominant position of the lamellar phase (compared to hexagonal) for any value of the model parameters.

Proceeding with the binodal lines we write the standard equilibrium conditions for the isotropic–lamellar coexistence (6.63) yielding

$$\begin{aligned} f_I &\simeq \left(\frac{L}{d}\right)^2 \exp\left(-\frac{Ld\gamma}{T}\right) , \\ f_L^{(1)} &\simeq \frac{1}{4}\,\frac{\kappa d\sqrt{N}}{a} . \end{aligned} \tag{6.78}$$

The same can be done for the equilibrium between the nematic and lamellar phases

$$\begin{aligned} f_N &\simeq 1 , \\ f_L^{(2)} &\simeq \frac{1}{1+\kappa N}\left[1 - \exp\left(\frac{-\epsilon + bd\gamma}{T} + \ln N^*\right)\right] . \end{aligned} \tag{6.79}$$

The resulting phase diagram is shown in Figure 6.7. A large part of it is occupied by the lamellar microphase, which appears above the $1/T_2$ point.

6.6. Discussion

In this chapter we addressed the peculiarities of the phase equilibria and microstructure formation of thermoreversible hairy-rod polymers. The main results are summarized in the phase diagrams Figure 6.4, 6.6 and 6.7.

We started from a blend of rods and coils, which are in general strongly incompatible, Figure 6.2a. In has been shown that thermoreversible association induces a significant compatibility enhancement: for the association energy beyond a certain value, $\epsilon > 2bw/d$, a partial compatibility is achieved at temperatures below T^*, (6.26), to the left from the stoichiometric point (see Figure 6.2b). The conversion parameter p is close to unity in the coil-rich phase and negligibly small in the rod-rich phase.

Furthermore, the compatibility region was proven to be unstable against microstructure formation. Due to mutual attraction between hairy-rod molecules in a melt of flexible coils, they tend to self-organize. Three types of microphases, namely H1 and H2 hexagonal and lamellar, can appear and coexist with each other as well as with the isotropic and nematic phase (see phase diagrams Figure 6.4, 6.6 and 6.7). The actual selection between the different microphases at any given temperature is a result of the competition between the "surface tension" γ-part of the free energy and the elastic stretching of the side chains: the first one is responsible for the tendency of the rods to stick together, whereas the second one, if the hairy-rod is densely grafted, prevents it. This competition leads to the hexagonal H1 phase being stable at relatively high temperatures. For somewhat lower temperatures it is followed by H2 and then by the lamellar microphases (Figure 6.4). Actually, depending on the value of the $\epsilon d/bw$ parameter, equations (6.73) and (6.74), three different sequences of microphases are possible. For quite small values, see (6.74), only a narrow strip of the lamellar microphase is present along with the nematic and isotropic phase, Figure 6.6b. If $\epsilon d/bw$ is large enough, (6.73), all three microstructures appear Figure 6.4. In the intermediate regime only two, H2 and lamellar, are possible. In many respects this situation resembles that of the covalently bonded system [147], where these three types of sequences were predicted as well.

A qualitatively different situation is observed in the $\kappa N < 1$ case: the grafting density is always low and the elastic part of the free energy is negligibly small. This immediately results in the fact that only the lamellar structure can be found Figure 6.7. Indeed, nothing prevents rods from the γ-driven tendency to keep the contact area with coils as small as possible. The lamellar phase first appears at the triple point T_2, (6.77), and then occupies the lion share of the diagram (we remind that for $\kappa N < 1$ the stoichiometric point $1/(1 + \kappa N) > 1/2$). Existence of the Figure 6.7 type phase diagram is in accordance with the few experimental data available [65, 115, 153–156]. In these experimental systems, briefly discussed in the Introduction, the κN parameter is definitely less than unity[1]. So, a lamellar structure is expected to be present along with the isotropic and nematic phase (in practice the latter might correspond to either a nematic or a crystalline phase), which is indeed observed experimentally [65, 154, 156].

[1] Backbone "unit" includes (2.5-pyridinediyl)(MSA) plus OG's head whereas a side chain consists of a relatively short OG's tail.

Appendix

6.A. Expressions for the chemical potentials and partial pressures

We define chemical potential and pressure as

$$\mu = \frac{\partial F}{\partial f} ,$$
$$P = f\frac{\partial F}{\partial f} - F .$$

Below we list the explicit expressions for the chemical potentials and partial pressures of the isotropic liquid (I), nematic (N), hexagonal H1 and H2 and lamellar (L) phases.

Isotropic liquid phase

$$\begin{aligned}\frac{\mu_I}{T} &= \frac{2L}{d}\left(\frac{w}{T}+s\right) + Mp\left[\ln N^* - \frac{\epsilon}{T}\right] \\ &\quad + M\left[p\ln p + (1-p)\ln(1-p)\right] + \ln f \\ &\quad - \frac{M(1+\kappa N p)}{N\kappa}\ln(1-f-f\kappa N p) \\ &\quad + \frac{3\kappa d^2}{32a^2} M p^2 \ln(\kappa N p)\, H\left(p - \frac{1}{\kappa N}\right) ,\end{aligned} \tag{6.80}$$

$$\frac{P_I}{T} = f - \frac{M}{N\kappa}\ln(1-f-f\kappa N p) + \frac{M}{N\kappa}(1-f-f\kappa N p) . \tag{6.81}$$

Nematic phase

$$\begin{aligned}\frac{\mu_N}{T} &= 2\ln\left(\frac{L}{d}\right) - \frac{M}{N\kappa}\frac{\mu_c}{T} + Mp\left[\ln N^* - \frac{\epsilon}{T}\right] \\ &\quad + M\left[p\ln p + (1-p)\ln(1-p)\right] + \ln f \\ &\quad - \frac{M(1+\kappa N p)}{N\kappa}\ln(1-f-f\kappa N p) ,\end{aligned} \tag{6.82}$$

$$\frac{P_N}{T} = f - \frac{M}{N\kappa}\frac{\mu_c}{T} - \frac{M}{N\kappa}\ln(1-f-f\kappa N p) + \frac{M}{N\kappa}(1-f-f\kappa N p) . \tag{6.83}$$

Hexagonal H1 phase

$$\begin{aligned}\frac{\mu_{H1}}{T} &= \frac{2L}{d}\left(\frac{w}{T}+s\right)+Mp\left[\ln N^{*}-\frac{\epsilon}{T}\right]\\ &+M\left[p\ln p+(1-p)\ln(1-p)\right]+2\ln\left(\frac{L}{d}\right)\\ &-\frac{M\left(1+\kappa Np\right)}{N\kappa}\ln\left(1-f-f\kappa Np\right)\\ &+\frac{3\kappa d^{2}}{32a^{2}}Mp^{2}\ln\left(\kappa Np\right)\\ &-\frac{3}{32}\frac{\kappa Mp^{2}d^{2}}{a^{2}}\left[3.457+1+\ln\left(\frac{a^{2}Nf}{d^{2}}\right)\right], \end{aligned} \tag{6.84}$$

$$\frac{P_{H1}}{T}=-\frac{M}{N\kappa}\ln\left(1-f-f\kappa Np\right)+\frac{M}{N\kappa}\left(1-f-f\kappa Np\right)-\frac{3}{32}f\frac{\kappa Mp^{2}d^{2}}{a^{2}}. \tag{6.85}$$

Hexagonal H2 phase

In the case of the H2 phase first the minimization upon Q has to be carried out.

$$\begin{aligned}\frac{1}{fT}\frac{\partial F_{H2}}{\partial Q} &= \frac{2L}{Q^{2}d}\left(\frac{w}{T}+s\right)+\frac{3\kappa d^{2}}{32a^{2}}Mp^{2}\ln\left(\kappa Np\right)\\ &-\frac{3}{32}\frac{\kappa Mp^{2}d^{2}}{a^{2}}\left[3.457-1+\ln\left(\frac{a^{2}Nf}{Qd^{2}}\right)\right]=0. \end{aligned} \tag{6.86}$$

If we neglect the lattice formation energy, the result (6.39) can be obtained. Chemical potential of the H2 hexagonal phase can be obtained as

$$\mu_{H2}=\left(\frac{\partial F}{\partial f}\right)_{Q}+\left(\frac{\partial F}{\partial Q}\right)_{f}\frac{\partial Q}{\partial f}=\left(\frac{\partial F}{\partial f}\right)_{Q}$$

and reads

$$\begin{aligned}\frac{\mu_{H2}}{T} &= \frac{L}{d}\left(\frac{w}{T}+s\right)\left(1+\frac{2}{Q}\right)+Mp\left[\ln N^{*}-\frac{\epsilon}{T}\right]\\ &\quad +M\left[p\ln p+(1-p)\ln(1-p)\right]+2\ln\left(\frac{L}{d}\right)\\ &\quad -\frac{M\left(1+\kappa Np\right)}{N\kappa}\ln\left(1-f-f\kappa Np\right)\\ &\quad +\frac{3\kappa d^{2}Q}{32a^{2}}Mp^{2}\ln\left(\kappa Np\right)\\ &\quad -\frac{3}{32}Q\frac{\kappa Mp^{2}d^{2}}{a^{2}}\left[3.457+1+\ln\left(\frac{a^{2}Nf}{Qd^{2}}\right)\right], \end{aligned} \tag{6.87}$$

$$\begin{aligned}\frac{P_{H2}}{T} &= -\frac{M}{N\kappa}\ln\left(1-f-f\kappa Np\right)\\ &\quad +\frac{M}{N\kappa}\left(1-f-f\kappa Np\right)-\frac{3}{32}f\frac{\kappa Mp^{2}d^{2}}{a^{2}}Q\,. \end{aligned} \tag{6.88}$$

Lamellar phase

$$\begin{aligned}\frac{\mu_{L}}{T} &= \frac{L}{d}\left(\frac{w}{T}+s\right)+Mp\left[\ln N^{*}-\frac{\epsilon}{T}\right]\\ &\quad +M\left[p\ln p+(1-p)\ln(1-p)\right]+2\ln\left(\frac{L}{d}\right)\\ &\quad -\frac{M\left(1+\kappa Np\right)}{N\kappa}\ln\left(\frac{H}{\xi}(1-f-f\kappa Np)\right)\\ &\quad +\frac{3\pi^{2}\kappa^{2}d^{2}}{32a^{2}}NMp^{3}-\frac{1.312M}{f^{*}}\left(\frac{p^{2}d^{2}}{\kappa a^{2}N^{2}}\right)^{1/3}, \end{aligned} \tag{6.89}$$

$$\begin{aligned}\frac{P_{L}}{T} &= -\frac{M}{N\kappa}\ln\left(\frac{H}{\xi}(1-f-f\kappa Np)\right)+\frac{M}{N\kappa}\left(1-f-f\kappa Np\right)\\ &\quad +0.227f^{*}M\left(\frac{pa^{2}}{\kappa^{2}d^{2}N}\right)^{1/3}-1.312M\left(\frac{p^{2}d^{2}}{\kappa a^{2}N^{2}}\right)^{1/3}. \end{aligned} \tag{6.90}$$

For H and ξ see (6.59) and (6.62).

Hexagonal H2 phase in the vicinity of the H2-Lam transition

The free energy is given by the following expression

$$\begin{aligned} F'_{H2} &= f\frac{L}{d}\left(\frac{w}{T}+s\right)\left(1+\frac{2}{Q}\right)+Mfp\left[\ln N^{*}-\frac{\epsilon}{T}\right] \\ &\quad +fM\left[p\ln p+(1-p)\ln(1-p)\right]+2f\ln\left(\frac{L}{d}\right) \\ &\quad +M\frac{1-f-f\kappa Np}{N\kappa}\ln\left(\frac{1-f-f\kappa Np}{e}\right)+F'^{(el)}_{H2}+U'_{H2}\,. \end{aligned} \tag{6.91}$$

Here $F'^{(el)}_{H2}$ is given by (6.22) and the energy of the lattice formation U'_{H2} is approximated by the corresponding term for the lamellar phase.

$$\begin{aligned} \frac{\mu'_{H2}}{T} &= \frac{L}{d}\left(\frac{w}{T}+s\right)\left(1+\frac{2}{Q}\right)+Mp\left[\ln N^{*}-\frac{\epsilon}{T}\right] \\ &\quad +M\left[p\ln p+(1-p)\ln(1-p)\right]+2\ln\left(\frac{L}{d}\right) \\ &\quad -\frac{M(1+\kappa Np)}{N\kappa}\ln(1-f-f\kappa Np) \\ &\quad +\frac{3\pi^2\kappa^2d^2}{32a^2}NMp^3-3\left(\frac{\pi\kappa}{4}\right)^3\frac{d^2N^2M}{Qa^2}p^4 \\ &\quad -\frac{1.312M}{f^{*}}\left(\frac{p^2d^2}{\kappa a^2N^2}\right)^{1/3}\,, \end{aligned} \tag{6.92}$$

$$\begin{aligned} \frac{P'_{H2}}{T} &= -\frac{M}{N\kappa}\ln(1-f-f\kappa Np)+\frac{M}{N\kappa}(1-f-f\kappa Np) \\ &\quad +0.227f^{*}M\left(\frac{pa^2}{\kappa^2d^2N}\right)^{1/3}-1.312M\left(\frac{p^2d^2}{\kappa a^2N^2}\right)^{1/3}\,. \end{aligned} \tag{6.93}$$

As it has been pointed out before, the minimization upon Q cannot be performed. Indeed

$$\frac{\partial F'_{H2}}{\partial Q}=-\frac{2fL}{d}\frac{1}{Q^2}+3\left(\frac{\pi\kappa}{4}\right)^3\frac{d^2N^2Mf}{Q^2a^2}p^4$$

so $\partial F'_{H2}/\partial Q = 0$ does not have roots $Q < \infty$ in the approximation used. In order to obtain it, a more precise approximation is needed for $F'^{(el)}_{H2}$ and U'_{H2}.

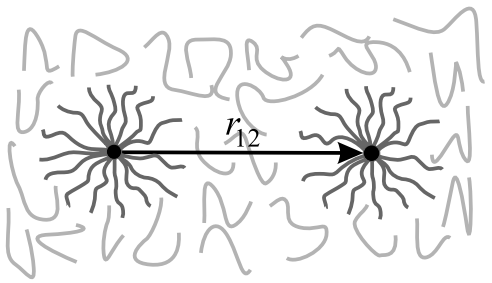

Figure 6.8: Two cylindrical micelles (a cross section)

6.B. Interaction between two cylindrical micelles

Let us consider the interaction between two cylindrical micelles in an otherwise homogeneous system, Figure 6.8. We assume the distance between them to be larger than the size of the corona, $r_{12} \gtrsim R_{corona}$. Therefore, the monomer density ϕ_{assoc} of the associated coils can be approximated as a sum of the densities ϕ_0 of the isolated micelles

$$\phi_{assoc}(\mathbf{r}) = \phi_0(\mathbf{r}) + \phi_0(\mathbf{r} - \mathbf{r}_{12})\,. \tag{6.94}$$

Attached to a rod chains still approximately obey Gaussian statistics, so that a probability to find the s-th monomer at the distance $\mathbf{r}$ from the 0-th one reads

$$p(\mathbf{r}, s) = \left(\frac{4\pi s a^2}{6}\right)^{-3/2} \exp\left[-\frac{6r^2}{4sa^2}\right].$$

Thus, the Fourier transform of ϕ_0 has the form

$$\phi_0(\mathbf{k}) = \mathcal{N}_s \frac{1 - \exp(-Nk^2a^2/6)}{k^2a^2/6}\,, \tag{6.95}$$

where $\mathcal{N}_s$ is the total number of side chains per micelle. Note, the free energy of the micelles interaction arises from the inhomogeneous distribution $\phi_{free}(\mathbf{r}) = 1 - \phi_{assoc}(\mathbf{r})$ of free coils in their surrounding. This energy can be calculated by the RPA method [105] and is given by the equation (6.27). Using (6.94) and (6.95) we obtain

$$\Delta\phi(\mathbf{k}) = \phi_0(\mathbf{k})\left(1 + \mathrm{e}^{-i\mathbf{k}\mathbf{r}_{12}}\right)\,, \tag{6.96}$$

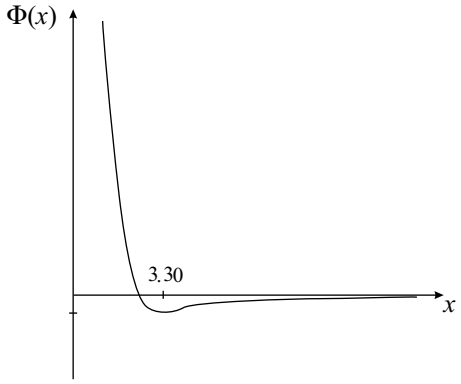

Figure 6.9: The interaction free energy of two cylindrical micelles separated by distance $r_{12} = xa\sqrt{N}$

and therefore the interaction energy (per unit length along the "backbone" of the micelle)

$$\frac{\Delta\mathcal{F}_{int}(r_{12})}{T} = \frac{3\mathcal{N}_s^2}{a^2}\Phi\left(\frac{r_{12}}{a\sqrt{N}}\right) , \tag{6.97}$$

where

$$\Phi(x) = \int_0^\infty \frac{q\,\mathrm{d}q}{(2\pi)^2}\,\frac{(1-\mathrm{e}^{-q^2})^2}{q^2-1+\mathrm{e}^{-q^2}}\,J_0(\sqrt{6}xq) \tag{6.98}$$

and $J_0(x) = \int_0^{2\pi} \mathrm{d}\varphi\,\mathrm{e}^{ix\cos\varphi}/(2\pi)$ is a Bessel function.

The function $\Phi(x)$ is schematically depicted in Figure 6.9. The micelles *attract* each other at large distances and the function reaches its minimum at $x = r_{12}/(a\sqrt{N}) \simeq 3.30$. This attraction is responsible for the superlattice formation as shown in section 6.4.1.

6.C. Free energy of the lattice formation

Let us start from a general formula for the free energy of the whole lattice (see (6.27) and [105, 130])

$$\frac{\mathcal{F}_{int}}{T} = \frac{\nu}{2N}\int \frac{1}{f_D\left(\frac{k^2a^2N}{6}\right)}\,|\Delta\phi(\mathbf{k})|^2\,\frac{\mathrm{d}\mathbf{k}}{(2\pi)^3} , \tag{6.99}$$

where $f_D(u)$ is the Debye scattering function

$$f_D(u) = \frac{2}{u^2}\left(u - 1 + \mathrm{e}^{-u}\right) \tag{6.100}$$

and $\Delta\phi(\mathbf{k})$ is the Fourier transform of the function $\phi_{free}(\mathbf{r}) - 1 = -\phi_{assoc}(\mathbf{r})$, ϕ_{free} and ϕ_{assoc} are monomeric densities of the free chains and chains attached to the rods.

Hexagonal lattice

We consider cylinders consisting of Q rods each and forming a hexagonal lattice (effectively 2D) with vertexes at the points $\mathbf{r}_{mn}$. Further, it is assumed [105, 130] that the density of the attached chains can be written as a sum of densities of virtually isolated cylinders, i.e. $\phi_{assoc}(\mathbf{r}) = \sum_{m,n} \phi_0(\mathbf{r} - \mathbf{r}_{mn})$, or, in other words,

$$\Delta\phi(\mathbf{k}) = -\phi_0(\mathbf{k}) \sum_{m,n} \mathrm{e}^{-i\mathbf{k}\mathbf{r}_{mn}} . \tag{6.101}$$

This immediately gives

$$|\Delta\phi(\mathbf{k})|^2 = \phi_0^2(\mathbf{k}) \sum_{s,t} \sum_{m,n} \mathrm{e}^{-i\mathbf{k}(\mathbf{r}_{mn}+\mathbf{r}_{st})} = \phi_0^2(\mathbf{k}) \mathcal{N}_{cells} \sum_{m,n} \mathrm{e}^{-i\mathbf{k}\mathbf{r}_{mn}} , \tag{6.102}$$

where $\mathcal{N}_{cells}$ is the total number of cells (or, equally, cylinders) in the system.

Function ϕ_0 is calculated for Gaussian chains forming cylindrical brush and reads

$$\phi_0(\mathbf{k}) = \mathcal{N}_s \frac{1 - \mathrm{e}^{-u}}{u} N . \tag{6.103}$$

Here $\mathcal{N}_s$ is the total number of the side chains forming a cylinder and $u = Nk^2a^2/6$.

For the further derivation the identity

$$\sum_{m,n} \mathrm{e}^{-i\mathbf{k}\mathbf{r}_{mn}} = \sum_{m,n} v' \delta\left(\mathbf{k} - \mathbf{b}_{mn}\right) \tag{6.104}$$

is used [157]. Here $\mathbf{b}_{mn}$ is a vector of a reciprocal lattice and v' is volume of its elementary cell.

If one considers a sample in the form of a cube with side $\mathcal{L}$, then the direct lattice elementary cell has dimensions $\ell \times \ell \times \mathcal{L}$, where ℓ is the period of the lattice ($\mathcal{L}$ will drop out from all final expressions). The cross section of this cell is depicted in Figure 6.10.

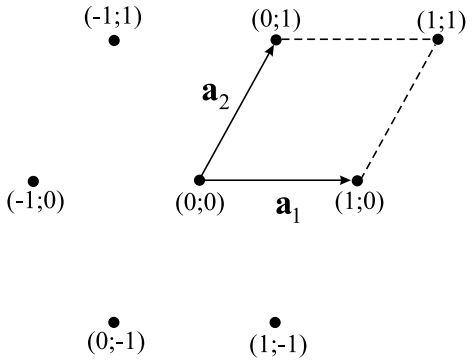

Figure 6.10: An elementary cell of a hexagonal lattice.

The lattice basis vectors $\mathbf{a}_1$ and $\mathbf{a}_2$ have Cartesian coordinates $\mathbf{a}_1 = (1;0)$ and $\mathbf{a}_2 = (1/2;\sqrt{3}/2)$ and any vector of the lattice can be represented as their linear combination

$$\mathbf{r}_{mn} = (m\mathbf{a}_1 + n\mathbf{a}_2)\ell.$$

Volume of the direct lattice cell reads

$$v = \frac{\sqrt{3}}{2}\mathcal{L}\ell^2 \,, \tag{6.105}$$

which means that volume of the reciprocal cell is

$$v' = \frac{(2\pi)^3}{v} = \frac{2(2\pi)^3}{\sqrt{3}}\frac{1}{\mathcal{L}\ell^2} \,. \tag{6.106}$$

The reciprocal lattice basis vectors have to be built from the condition

$$\begin{aligned} \mathbf{a}_1\mathbf{b} &= 2\pi p_1 \\ \mathbf{a}_2\mathbf{b} &= 2\pi p_2 \end{aligned} \tag{6.107}$$

for any vector $\mathbf{b} = p_1\mathbf{b}_1 + p_2\mathbf{b}_2$ of the reciprocal lattice [157]. Here $\mathbf{b}_1$ and $\mathbf{b}_2$ are the basis vectors of the reciprocal lattice and $p_{1,2}$ are any integer numbers. From the set of equations (6.107) one obtains

$$\mathbf{b}_1 = 2\pi\left(1; -\frac{1}{\sqrt{3}}\right) \tag{6.108}$$

$$\mathbf{b}_2 = 2\pi\left(0; \frac{2}{\sqrt{3}}\right) . \tag{6.109}$$

Now plugging expressions (6.100), (6.102) - (6.104), (6.106),and (6.108) into (6.99) we obtain the free energy of the system in the form

$$\frac{\mathcal{F}_{int}^{(HEX)}}{T} = \frac{\mathcal{N}_{cells}\mathcal{N}_s^2}{2\sqrt{3}} \frac{N\nu}{\mathcal{L}\ell^2} \sum_{m,n} \frac{(1-\mathrm{e}^{-u_{mn}})^2}{u_{mn}-1+\mathrm{e}^{-u_{mn}}}\,, \tag{6.110}$$

where

$$u_{mn} = \frac{2}{9}\left(\frac{2\pi N^{1/2}a}{\ell}\right)^2 (m^2+n^2-mn)\,. \tag{6.111}$$

Introducing $x = (2/9)\left(2\pi N^{1/2}a/\ell\right)^2$ one can rewrite (6.110)

$$\frac{\mathcal{F}_{int}^{(HEX)}}{T} = \frac{9\mathcal{N}_{cells}\mathcal{N}_s^2}{16\pi^2\sqrt{3}} \frac{\nu}{a^2\mathcal{L}} \sum_{m,n} x \frac{\left(1-\mathrm{e}^{-x(m^2+n^2-mn)}\right)^2}{x(m^2+n^2-mn)-1+\mathrm{e}^{-x(m^2+n^2-mn)}}\,. \tag{6.112}$$

The sum in (6.112) represents the gain in the free energy of the system due to inhomogeneity in the free coils distribution and corresponds to the first addend in (6.28). To obtain the *interaction* energy of the hexagonal lattice with a period ℓ one has to subtract from (6.112) the energy of the lattice with infinitely long period $\ell \to \infty$, i.e. $x = x_\infty \to 0$.

Below we present the evaluation of the sum (6.112)

$$\sum_{m=-\infty}^{+\infty}\sum_{n=-\infty}^{+\infty} \frac{x(1-\mathrm{e}^{-x(m^2+n^2-mn)})^2}{x(m^2+n^2-mn)-1+\mathrm{e}^{-x(m^2+n^2-mn)}} =$$

$$2 + 4\sum_{n=1}^{+\infty} \frac{x(1-\mathrm{e}^{-xn^2})^2}{xn^2-1+\mathrm{e}^{-xn^2}} +$$

$$2\sum_{n=1}^{+\infty}\sum_{m=1}^{+\infty}\Big(\frac{x(1-\mathrm{e}^{-x(m^2+n^2-mn)})^2}{x(m^2+n^2-mn)-1+\mathrm{e}^{-x(m^2+n^2-mn)}} +$$

$$\frac{x(1-\mathrm{e}^{-x(m^2+n^2+mn)})^2}{x(m^2+n^2+mn)-1+\mathrm{e}^{-x(m^2+n^2+mn)}}\Big)\,.$$

The last sum for $x > 0$ and $n, m = 1, \ldots, \infty$ can be approximated as

$$\sum_{n=1}^{+\infty}\sum_{m=1}^{+\infty}\left(\frac{1}{m^2+n^2-mn} + \frac{1}{m^2+n^2+mn}\right) = \sum_{n=1}^{+\infty}\left(\sum_{m=-\infty}^{+\infty}\frac{1}{m^2+n^2-mn} - \frac{1}{n^2}\right)\,.$$

The summation over m can be solved using the following formula [158] ($f(n)$ is an arbitrary function analytical everywhere in the complex plane $\mathbb{C}$, except a finite number of poles z_i):

$$\sum_{m=-\infty}^{+\infty} f(m) = -\pi \sum_{z_i} \operatorname{res}\left(f(z)\cot z\right).$$

Therefore

$$\sum_{m=-\infty}^{+\infty} \frac{1}{m^2+n^2-mn} = \frac{2\pi}{n\sqrt{3}} \frac{\sinh(\pi n\sqrt{3})}{\cosh(\pi n\sqrt{3})-(-1)^n}.$$

Also considering that $\sum_{n=1}^{\infty} 1/n^2 = \pi^2/6$ we obtain for the sum

$$2 + \frac{\pi^2}{3} + \frac{4\pi}{\sqrt{3}} \sum_{n=1}^{\infty} \frac{1}{n} \frac{\sinh(\pi n\sqrt{3})}{\cosh(\pi n\sqrt{3})-(-1)^n}.$$

At this point one has to separate diverging part in the expression under the sum sign

$$2 + \frac{\pi^2}{3} + \frac{4\pi}{\sqrt{3}} \sum_{n=1}^{\infty} \frac{1}{n} \left(\frac{\sinh(\pi n\sqrt{3})}{\cosh(\pi n\sqrt{3})-(-1)^n} - 1 \right) + \frac{4\pi}{\sqrt{3}} \sum_{n=1}^{\infty} \frac{1}{n} = 5.23 + \frac{4\pi}{\sqrt{3}} \sum_{n=1}^{\infty} \frac{1}{n}.$$

The sum has to be computed for $x \to 0$ as well and subtracted from the previous expression. Taking into account that $x_\infty \to 0$, we can introduce new variables $y_1 = \sqrt{x_\infty} m$ and $y_2 = \sqrt{x_\infty} n$ and replace the summation by integral (c.f. the second addend in (6.28))

$$\sum_{n,m=-\infty}^{+\infty} \frac{x_\infty (1-\mathrm{e}^{-x_\infty(m^2+n^2-mn)})^2}{x_\infty(m^2+n^2-mn) - 1 + \mathrm{e}^{-x_\infty(m^2+n^2-mn)}} =$$

$$2\int_0^{+\infty} \mathrm{d}y_1 \int_{-\infty}^{+\infty} \mathrm{d}y_2 \frac{(1-\mathrm{e}^{-(y_1^2+y_2^2-y_1y_2)})^2}{(y_1^2+y_2^2-y_1y_2) - 1 + \mathrm{e}^{-(y_1^2+y_2^2-y_1y_2)}} =$$

$$2\int_0^{1} \mathrm{d}y_1 \int_{-\infty}^{+\infty} \mathrm{d}y_2 \big(...\big) + 2\int_1^{\infty} \mathrm{d}y_1 \int_{-\infty}^{+\infty} \mathrm{d}y_2 \big(...\big).$$

The first integral can be solved numerically and is approximately equal to 5.05. After

treating the last integral as

$$\int_1^{\infty} \mathrm{d}y_1 \int_{-\infty}^{+\infty} \mathrm{d}y_2 \big(...\big) =$$
$$\int_1^{\infty} \mathrm{d}y_1 \int_{-\infty}^{+\infty} \mathrm{d}y_2 \left[\frac{(1-\mathrm{e}^{-(y_1^2+y_2^2-y_1y_2)})^2}{(y_1^2+y_2^2-y_1y_2)-1+\mathrm{e}^{-(y_1^2+y_2^2-y_1y_2)}} - \frac{1}{y_1^2+y_2^2-y_1y_2} \right] +$$
$$\int_1^{\infty} \mathrm{d}y_1 \int_{-\infty}^{+\infty} \mathrm{d}y_2 \frac{1}{y_1^2+y_2^2-y_1y_2} = 0.8074 + \int_1^{\infty} \mathrm{d}y_1 \frac{2\pi}{\sqrt{3}y_1}$$

one can see that both the sum (appeared above) and the integral have the same type of divergence. Subtracting one from the other we obtain

$$\sum_1^{\infty} \frac{1}{n} - \int_1^{\infty} \frac{\mathrm{d}y}{y} = \lim_{M^*\to\infty} \left(\sum_1^{M^*} \frac{1}{n} - \int_1^{\sqrt{x}M^*} \frac{\mathrm{d}y}{y} \right) = \gamma_E - \ln\left(\frac{\sqrt{2}}{3} \frac{2\pi N^{1/2} a}{\ell} \right),$$

where $\gamma_E \approx 0.577$ is Euler γ [158].

To get rid of variables $\mathcal{N}$ and $\mathcal{L}$ we notice that $\mathcal{N}_s = QMp\mathcal{L}/L$ and $\mathcal{N}_{cells} = 2V/(\sqrt{3}\mathcal{L}\ell^2)$ (here V is the total volume of the sample).

Finally we have to rewrite the total free energy of the lattice as energy per rod. This can be done multiplying the free energy density by the rod's volume. Also the period of the structure ℓ has to be expressed in terms of the volume fraction of rods f as

$$\ell^2 = \frac{1}{2\sqrt{3}} \frac{\pi d^2 Q}{f}.$$

All this together gives (6.30)

$$\frac{U^{(HEX)}}{T} = \frac{3}{32} \frac{\kappa Q M p^2 d^2}{a^2} f \left[-3.456 + \ln \frac{Qd^2}{fNa^2} \right]. \tag{6.113}$$

Tetragonal lattice

The interaction energy for a tetragonal lattice can be calculated using the same approach as described above. We just sketch all the necessary steps here.

A tetragonal 2D lattice is characterized by a set of vectors, Figure 6.11

$$\mathbf{a}_1 = (1;0)$$
$$\mathbf{a}_2 = (0;1)$$

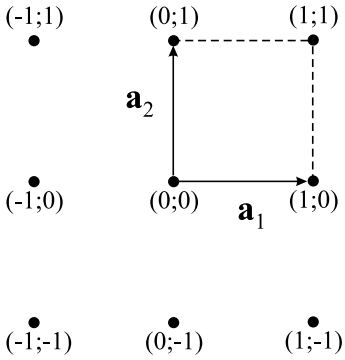

Figure 6.11: An elementary cell of a tetragonal lattice.

so that an elementary cell's volume reads $v = \mathcal{L}\ell^2$. A reciprocal lattice in this case is also tetragonal with basis vectors

$$\mathbf{b}_1 = 2\pi(1;0)$$
$$\mathbf{b}_2 = 2\pi(0;1)$$

and volume $v' = (2\pi)^3/(\mathcal{L}\ell^2)$. Using (6.99) one concludes that the free energy of the lattice has the form

$$\frac{\mathcal{F}_{int}^{(TET)}}{T} = \frac{3\mathcal{N}_{cells}\mathcal{N}_s^2}{2(2\pi)^2}\frac{\nu}{\mathcal{L}a^2}\sum_{m,n} x\frac{\left(1-\mathrm{e}^{-x(m^2+n^2)}\right)^2}{x(m^2+n^2)-1+\mathrm{e}^{-x(m^2+n^2)}}\,, \tag{6.114}$$

where $x = \left(2\pi N^{1/2}a/\ell\right)^2/6$.
The summation leads to

$$\sum_{m,n} x\frac{\left(1-\mathrm{e}^{-x(m^2+n^2)}\right)^2}{x(m^2+n^2)-1+\mathrm{e}^{-x(m^2+n^2)}} \simeq$$
$$2 + 2\sum_{n=1}^{\infty}\frac{1}{n^2} + 2\sum_{n=1}^{\infty}\sum_{m=-\infty}^{\infty}\frac{1}{n^2+m^2} = 2 + 2\,\frac{\pi^2}{6} + 2\sum_{n=1}^{\infty}\frac{\pi}{n}\coth(\pi n) =$$
$$2 + \frac{\pi^2}{3} + 2\pi\sum_{n=1}^{\infty}\frac{1}{n}\left[\coth(\pi n)-1\right] + 2\pi\sum_{n=1}^{\infty}\frac{1}{n} = 5.3134 + 2\pi\sum_{n=1}^{\infty}\frac{1}{n}\,.$$

The term for $x \to 0$ has to be subtracted from the expression above

$$\sum_{n,m=-\infty}^{+\infty} \frac{x_\infty(1-\mathrm{e}^{-x_\infty(m^2+n^2)})^2}{x_\infty(m^2+n^2)-1+\mathrm{e}^{-x_\infty(m^2+n^2)}} =$$

$$2\int_0^{+\infty}\mathrm{d}y_1\int_{-\infty}^{+\infty}\mathrm{d}y_2\frac{(1-\mathrm{e}^{-(y_1^2+y_2^2)})^2}{(y_1^2+y_2^2)-1+\mathrm{e}^{-(y_1^2+y_2^2}} =$$

$$2\int_0^{1}\mathrm{d}y_1\int_{-\infty}^{+\infty}\mathrm{d}y_2\Big(...\Big)+2\int_1^{\infty}\mathrm{d}y_1\int_{-\infty}^{+\infty}\mathrm{d}y_2\Big(...\Big) =$$

$$2\times 4.89+2\left[0.63+\int_1^{\infty}\mathrm{d}y_1\int_{-\infty}^{+\infty}\frac{\mathrm{d}y_2}{y_1^2+y_2^2}\right] = 11.05+2\int_1^{\infty}\frac{\pi\,\mathrm{d}y}{y}\,.$$

Finally, substituting $\mathcal{N}_{cells}$, $\mathcal{N}_s$ and $\ell^2 = \pi d^2/(4f)$ we get per volume of one rod

$$\frac{U^{(TET)}}{T} = \frac{3}{32}\,\frac{\kappa M p^2 d^2}{a^2} f\left[-2.798+\ln\frac{d^2}{fNa^2}\right]. \tag{6.115}$$

As one can see from the comparison with (6.113), the lattice energy of the tetragonal structure is always higher than for hexagonal H1 phase. This is the primary reason why the tetragonal microphase is always suppressed by the hexagonal one.

Lamellar structure ($\kappa N < 1$)

Let us start again from the expression (6.99). In the case of a lamellar structure we deal with a 1D lattice. Following the outline of the previous section we first calculate $|\Delta\phi(\mathbf{k})|^2$, which has exactly the same form (6.101)-(6.103) as before. Cartesian coordinates of the vectors of the direct $\mathbf{a} = (1;0;0)$ and reciprocal $\mathbf{b} = 2\pi(1;0;0)$ lattices can be easily found. Volume of the reciprocal cell reads $v' = (2\pi)^3/(\ell\mathcal{L}^2)$.

Therefore, the free energy is obtained as

$$\frac{\mathcal{F}_{int}^{(LAM)}}{T} = \frac{\mathcal{N}_{cells}\mathcal{N}_s^2}{4}\frac{N\nu}{\mathcal{L}^2 l}\sum_n \frac{(1-\mathrm{e}^{-xn^2})^2}{xn^2-1+\mathrm{e}^{-xn^2}} =$$

$$\frac{\mathcal{N}_{cells}\mathcal{N}_s^2}{4}\frac{N\nu}{\mathcal{L}^2}\frac{\sqrt{6}}{2\pi N^{1/2}a}\sum_n \sqrt{x}\frac{(1-\mathrm{e}^{-xn^2})^2}{xn^2-1+\mathrm{e}^{-xn^2}}\,, \tag{6.116}$$

where $x = \left(2\pi N^{1/2} a/\ell\right)^2/6$.
Summation leads to

$$\sum_{n=-\infty}^{+\infty} \sqrt{x}\frac{(1-\mathrm{e}^{-xn^2})^2}{xn^2-1+\mathrm{e}^{-xn^2}} = 2\sqrt{x} + 2\sqrt{x}\sum_{n=1}^{+\infty}\frac{(1-\mathrm{e}^{-xn^2})^2}{xn^2-1+\mathrm{e}^{-xn^2}} \simeq$$

$$2\sqrt{x} + 2\sqrt{x}\sum_{n=1}^{+\infty}\frac{1}{xn^2} = 2\sqrt{x} + \frac{\pi^2}{3\sqrt{x}}\,.$$

For $x = x_\infty \to 0$:

$$\sum_{n=-\infty}^{+\infty} \sqrt{x_\infty}\frac{(1-\mathrm{e}^{-x_\infty n^2})^2}{x_\infty n^2-1+\mathrm{e}^{-x_\infty n^2}} = \int_{-\infty}^{+\infty} \mathrm{d}y \frac{(1-\mathrm{e}^{-y^2})^2}{y^2-1+\mathrm{e}^{-y^2}} \simeq 5.644.$$

Rewriting (6.116) after summation one obtains for the free energy per rod (6.75)

$$\frac{U^{(LAM)}}{T} = \frac{\pi^2}{128}\,\frac{M\kappa p^2 d^2}{a^2} + \frac{Mf\kappa p^2 d\sqrt{N}}{8a}\left[-1.728 + \frac{af\sqrt{N}}{d}\right]. \qquad (6.117)$$